J Mater Sci (2007) 42:2684–2689
DOI 10.1007/s10853-006-1368-x

Preparation and characterization of L-cystine and L-cysteine intercalated layered double hydroxides

Min Wei · Jian Guo · Zhiyu Shi · Qi Yuan · Min Pu · Guoying Rao · Xue Duan

Received: 10 August 2005 / Accepted: 22 February 2006 / Published online: 4 January 2007

Abstract L-cystine and L-cysteine have been intercalated into magnesium–aluminum layered double hydroxide by the methods of coprecipitation and ion-exchange. The structure and composition of the intercalated materials have been characterized by X-ray diffraction (XRD), Fourier transform infrared (FT-IR) spectroscopy and elemental analysis. For L-cysteine intercalated composites, two kinds of well-crystallized materials with different basal spacing were obtained, as a result of the different charge on an ion and orientation of the gallery anions. The schematic models of the intercalation structures were proposed. In addition, the thermal decomposition of L-cystine and L-cysteine intercalated LDHs has been investigated by means of thermogravimetry and differential thermal analysis (TG-DTA).

Introduction

Layered double hydroxides, which are widely known as host–guest materials, have received considerable attention due to their special intercalation properties. LDHs can be represented by the general formula $[M^{II}_{1-x}M^{III}_x(OH)_2]^{x+}(A^{n-})_{x/n} \cdot mH_2O$ [1], where M^{II}, M^{III} are di- and tri-valent metal cations respectively; A^{n-} is an exchangeable inorganic or organic anion, and the x value, i.e., the substitution rate, is equal to the molar ratio $M^{III}/(M^{II}+ M^{III})$. LDHs consist of positively charged metal hydroxide layers, in which the anions (along with water) are stabilized in order to compensate the positive layer charges. Various kinds of inorganic or organic anions have been introduced between the hydroxide layers by simple ion-exchange reaction or coprecipitation, e.g., inorganic acids [2], organic acids [3], anionic polymers [4], cyclodextrin [5], and reduced C_{60} [6]. The attractive feature of such materials is that they serve as a template for the formation of supramolecular structures [7]. The host layers can impose restricted geometry on the interlayer guests leading to enhanced control of stereochemistry, rates of reaction, and product distributions. These layered solids based upon the alternation of inorganic and organic layers have received considerable attention, because of their many practical applications in areas such as heterogeneous catalysis [8, 9], optical materials [10, 11], biomimetic catalysis [12, 13] and separation science [14, 15].

In recent years, much attention has been paid to the intercalation of biomolecules or pharmaceutical agents into LDHs, such as amino acids [16, 17], nucleoside monophosphates and deoxyribonucleic acid [18], c-antisense oligonucleotide (As-myc) [19], nucleoside mono phosphates and deoxyribonucleic acid (DNA) [19], vitamin (A,C,E) [20]. LDHs is biocompatible and has found pharmaceutical applications as an antacid, or as an ingredient in sustained-release pharmaceuticals containing nifedipine, for stabilizing pharmaceutical compositions and for preparing aluminium magnesium salts of antipyretic, analgesic and antiinflammatory drugs [21]. Recently, the intercalation of amino acids

M. Wei · J. Guo · Z. Shi · Q. Yuan · M. Pu · G. Rao · X. Duan (✉)
State Key Laboratory of Chemical Resource Engineering, Beijing University of Chemical Technology, Beijing 100029, P. R. China
e-mail: duanx@mail.buct.edu.cn

into LDHs has attracted much interest of researchers. There have been some reports on the intercalation of amino acids into LDHs, such as glutamic acid [22], tyrosine [23], and phenylalanine [24]. In the present work, L-cystine and L-cysteine (represented as L-Cys and L-CysH, respectively) have been intercalated into the layers of LDHs for the first time, and the structure and composition of the intercalated materials have been characterized by XRD, FT-IR and elemental analysis. Moreover, the relationship between the anion orientation and the charge on an ion of L-CysH intercalated LDH has been studied. It has been known that some biomolecular chiral substances are unstable and their optical activity is readily lost by racemization under relatively mild conditions [25], so the biomolecule intercalated LDHs hybrids are expected for the developing new gene reservoir and carrier. Therefore, there is a potential application on regarding layered double hydroxides as ''molecule container'' to deposit and transport unstable chiral molecules.

Experimental

Preparation of L-Cys/LDH

The L-Cys/LDH was prepared by the method of coprecipitation. The matched molar ratio of Mg^{2+}/Al^{3+}/OH^-/L-Cys was 2.0/1.0/8.0/1.0. A solution of Mg$(NO_3)_2 \cdot 6H_2O$ (12.8 g, 0.05 mol) and Al$(NO_3)_3 \cdot 9H_2O$ (9.38 g, 0.025 mol) in 100 mL deionized water was slowly added dropwise to a 100 mL solution of NaOH (8.0 g, 0.20 mol) and L-Cys (6.0 g, 0.025 mol) with vigorous agitation under a nitrogen atmosphere. The value of the pH at the end of addition was adjusted to 10.0 by further addition of 2.4 mol L^{-1} NaOH solution. The reaction mixture was subsequently heated at 65 °C for 24 h, washed with hot deionized water and dried at 70 °C for 24 h. Elemental analysis (ICP) gave Mg: 13.89%, Al: 7.74%, C: 9.84%, N: 3.98%, H: 4.83%, S: 8.43%.

Preparation of L-CysH/LDH

L-CysH LDHs with different basal spacing were synthesized by the method of coprecipitation and ion exchange, respectively.

Sample 1: The matched molar ratio of Mg^{2+}/Al^{3+}/OH^-/L-CysH was 2.0/1.0/6.8/1.0. A solution of Mg$(NO_3)_2 \cdot 6H_2O$ (12.8 g, 0.05 mol) and Al$(NO_3)_3 \cdot 9H_2O$ (9.38 g, 0.025 mol) in 100 mL deionized water was slowly added dropwise to a 100 mL solution of NaOH (6.8 g, 0.17 mol) and L-CysH (3.025 g, 0.025 mol) with vigorous agitation under nitrogen atmosphere. The solution pH at the end of addition was 10.5. After addition, the reaction mixture was heated at 65 °C for 24 h, washed with hot deionized water and dried at 70 °C for 24 h. Elemental analysis (ICP) found Mg: 14.98%, Al: 8.26%, C: 5.94%, N: 2.27%, H: 4.92%, S: 4.27%.

Sample 2: The precursor $[Mg_4Al_2(OH)_{12}](NO_3)_2 \cdot 4H_2O$, (Mg/Al-$NO_3$ LDH) was synthesized by a procedure similar to that described previously [1]. The L-CysH/LDH was obtained by the method of ion-exchange. A 100 mL solution of L-CysH (6.05 g, 0.05 mol) in deionized water was added to a suspension of Mg/Al-NO_3 LDH (ca. 0.025 mol) in water, and the value of the pH was adjusted to 8.5 by further addition of 2.4 mol L^{-1} NaOH solution. The reaction mixture was subsequently heated at 65 °C under a nitrogen atmosphere for 12 h, washed with hot deionized water and dried at 70 °C for 24 h. Elemental analysis (ICP) found Mg: 15.64%, Al: 8.74%, C: 8.87%, N: 3.42%, H: 5.50%, S: 6.35%.

Characterization

Powder X-ray diffraction (XRD) measurements were performed on a Rigaku XRD-6000 diffractometer, using CuKα radiation (λ = 0.154 nm) at 40 kV, 30 mA, a scanning rate of 0.02°/s, and a 2θ angle ranging from 3° to 70°.

Fourier transform infrared (FT-IR) spectra were recorded using a Vector22 (Bruker) spectrophotometer in the range of 4,000–400 cm^{-1} with 2 cm^{-1} resolution. The standand KBr disk (1 mg of sample in 100 mg of KBr) was used.

Thermogravimetric analysis and differential thermal analysis (TG-DTA) were measured on a PCT-1A thermal analysis system with a heating rate of 10 °C/min in air.

Elemental analysis was performed by inductively coupled plasma (ICP-ES) emission spectroscopy on a Shimadzu ICPS-7500 instrument. C, H, N content was determined using an Elementarvario elemental analysis instrument.

Results and discussion

Crystal structure of L-Cys/LDH and L-CysH/LDH

The XRD patterns of L-Cys/LDH and L-CysH/LDH (Sam 1 and Sam 2) are shown in Fig. 1. In each case, the reflections can be indexed to a hexagonal lattice with *R*-3m rhombohedral symmetry, with a series of

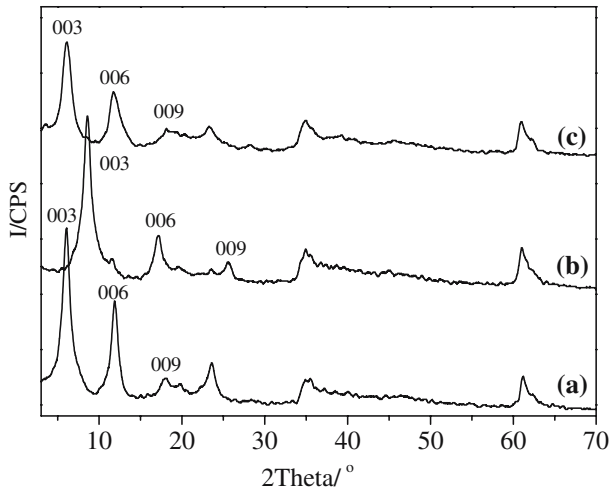

Fig. 1 Powder XRD patterns of (**a**) L-Cys/LDH, (**b**) L-CysH/LDH (Sam 1) and (**c**) L-CysH/LDH (Sam 2)

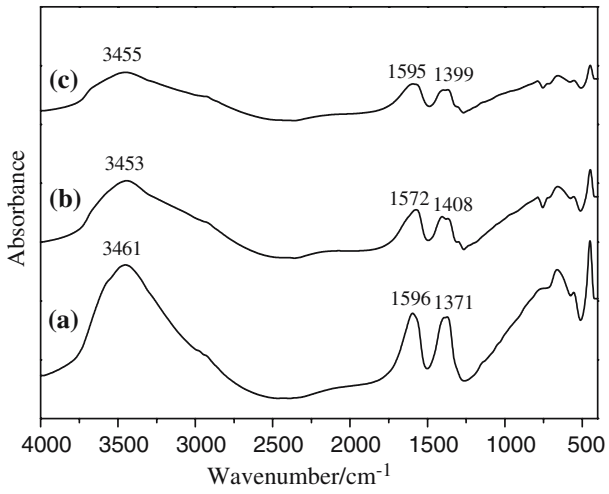

Fig. 2 FT-IR spectra of (**a**) L-Cys/LDH, (**b**) L-CysH/LDH (Sam 1) and (**c**) *L*-CysH/LDH (Sam 2)

(00*l*) peaks appearing as narrow, symmetric, strong lines at low angle, corresponding to the basal spacing and higher order reflections. This is commonly used for the description of LDH structures [26]. The main diffraction peaks of the L-Cys intercalated LDH appear at 6.04° (003), 11.88° (006), and 17.91° (009) (Fig. 1a). In addition, the peak at 23.55° is most likely due to the (006) reflection of the Mg–Al–CO_3 LDH phase. The same peak can be both observed in XRD patterns of L-CysH/LDH samples (Fig. 1b, c). Furthermore, the shoulder at 11.05° 2θ in Fig. 1b corresponds to the (003) reflection of Mg–Al–CO_3 LDH, while this peak was overlapped by the (006) reflection of the intercalates in L-Cys/LDH (Fig. 1a) and Sam 2 (Fig. 1c). This indicates that there is some separate Mg–Al–CO_3 LDH phase mixed in the three intercalated materials. For L-Cys/LDH and L-CysH/LDH (Sam 1 and Sam 2), the values of d_{003} are 1.46, 1.03 and 1.44 nm, respectively. The two samples of L-CysH intercalated LDH exhibit different basal spacing, which is due to the reason that the value of basal spacing is related to not only the guest size, but also the charge on an ion and orientation of the gallery anion. This will be further discussed in the next section.

Investigation of the host–guest interaction by FT-IR spectroscopy

Figure 2 displays the Infrared spectra of L-Cys/LDH and L-CysH/LDH (Sam 1 and Sam 2). The broad bands centered at 3461, 3453 and 3455 cm^{-1} in Fig.2a, b, c correspond to the O–H stretching vibration of surface and interlayer water molecules [27], which are found at lower frequency in LDHs compared with the O–H stretch in free water at 3600 cm^{-1} [28]. This is attributed to the formation of hydrogen bonding of interlayer water with the different guest anions as well as with the hydroxide groups of the layers. The asymmetric and symmetric stretching vibrations of alkyl carboxylate groups are observed at 1596, 1371 cm^{-1} (Fig. 2a), at 1572, 1408 cm^{-1} (Fig. 2b) and at 1595, 1399 cm^{-1} (Fig. 2c), respectively. Compared with carboxylic acid (~1,700 and 1,500 cm^{-1}), both the two peaks of carboxylate group shifted to the low frequency. The difference between the asymmetric and symmetric stretching vibration frequencies ($\Delta\nu$ values are 225, 164 and 196 cm^{-1} for the three samples, respectively) gives information about the symmetry of the interaction between the carboxylate group and the hydroxylated layers, which is similar to salt-like compounds [28, 29]. Additionally, the difference between the two $\Delta\nu$ values of the same guest L-CysH intercalated LDHs (Sam 1 and Sam 2) might indicate that there is some difference in the interaction of the two intercalated samples between guest anions and host layers, which relates to the different anion charge and orientation of interlayer guests. This will be discussed in the following section. The absorption band of co-existed CO_3^{2-} (~1,364 cm^{-1}) in all three samples might be overlapped by that of symmetric stretching vibration of R–COO^-, accounting for their broadened bands. The bands at 777, 667, 555, 449 cm^{-1} (Fig. 2a), 790, 667, 555, 449 cm^{-1} (Fig. 2b), and at 776, 663, 556, 448 cm^{-1} (Fig. 2c) are assigned to the M–O–M skeletal stretching and M–OH bending vibrations in the brucite-like sheets [28], respectively.

Schematic models of L-Cys/LDH and L-CysH/LDH

The ionization of L-Cys includes three steps in water arising from the presence of the two carboxyl groups and one amino group in its structure. The values of pK_a of L-Cys are: pK_{a1} < 1.00 (α-COOH); pK_{a2} = 2.10 (R-COOH); pK_{a3} = 8.71 (R-NH_3^+) [30], respectively. Based on the experimental condition for L-Cys/LDH with the aging solution pH at 10.0, the value of distribution coefficient of divalent anion (δ) can be calculated as $\delta > 90\%$, thus L-Cys exists mainly as divalent anion $^-OOCCHNH_2CH_2SSCH_2NH_2CHCOO^-$ during the aging process. Although the degree of ionization of the anions in solution is not necessarily the same as that of within the interlayer (ionic hydration occurs generally in solution), the concentration of anions with different charge has an influence on the intercalation process anyway. As shown in XRD results, the d_{003} of L-Cys/LDH is 1.46 nm. If the thickness of the LDH layer (0.48 nm) [29] is subtracted from the basal spacing, the gallery height is calculated to be 0.98 nm, which is a little smaller than the length of the L-Cys anion (1.05 nm, calculated by the method of molecular mechanics). Comparison of the length of the L-Cys anion with the gallery height suggests that L-Cys anions are accommodated approximately vertically in the interlayer region as a monolayer with the two carboxyl groups of individual anions attracted electrostatically to upper and lower hydroxide layers. The schematic representation of the possible arrangement for L-Cys/LDH is shown in Fig. 3a (Chemwindow 6.0).

The basal spacings of the two samples of L-CysH/LDH (Sam 1and Sam 2) prepared by different methods are different, which is due to the different charge on the ion and orientations of the gallery anion. The values of pK_a of L-CysH are: pK_{a1} = 1.96 (α-COOH); pK_{a2} = 8.18 (α-NH_3^+); pK_{a3} = 10.28 (R–SH) [30], respectively. According to the experimental condition for Sam 1 with the aging solution pH at 10.5, the value of distribution coefficient of divalent anion (δ) can be calculated as $\delta = 62\%$, thus L-CysH exists mainly as divalent anion $^-OOCCHNH_2CH_2S^-$ during the aging process. Taking into account the d_{003} of Sam 1 (1.03 nm) and the thickness of the LDH hydroxide basal layer (0.48 nm), the gallery height is calculated to be 0.55 nm, which is approximately equal to the length of the L-CysH anion (0.56 nm, calculated by molecular mechanics). This indicates that the orientation of L-CysH anions in Sam 1 is similar to that of L-Cys/LDH, i.e., they are accommodated vertically in the interlayer region as a monolayer with the two negative groups of individual anions attracted electrostatically to upper and lower hydroxide layers, as depicted in Fig. 3b.

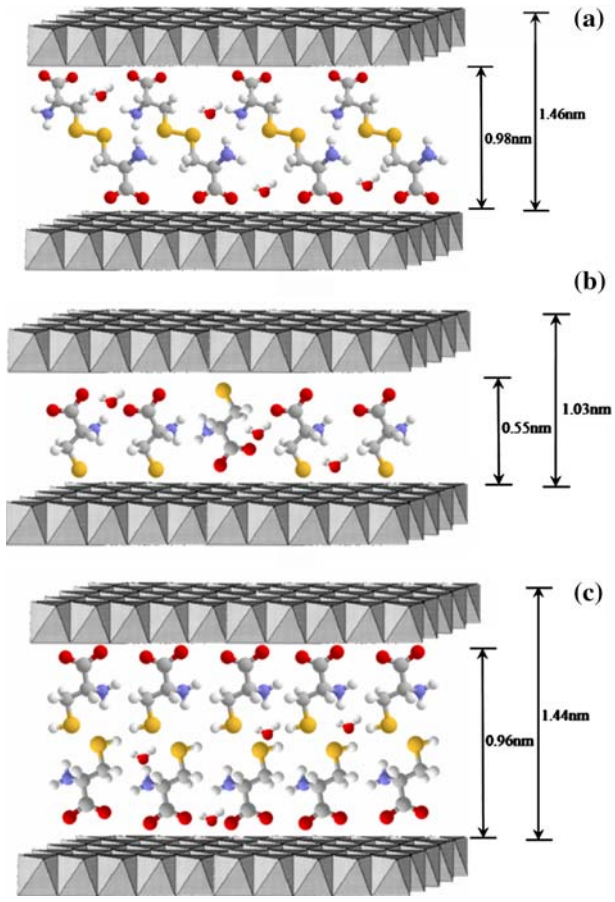

Fig. 3 Schematic representations of the possible arrangements for (**a**) L-Cys/LDH, (**b**) L-CysH/LDH (Sam 1) and (**c**) L-CysH/LDH (Sam 2)

The case is different for Sam 2. Based on the experimental condition for Sam 2 with the ion exchange solution pH at 8.5, the value of distribution coefficient of monovalent anion (δ) is calculated as $\delta = 83\%$, thus L-CysH exists mainly as monovalent anion $^-OOCCHNH_2CH_2SH$ during the intercalation process. When the thickness of the LDH hydroxide basal layer (0.48 nm) is subtracted from the basal spacing (1.44 nm), the gallery height is calculated to be 0.96 nm, which is approximately two times of the length of the L-CysH anion (0.56 nm). Comparison between the two values might suggest that L-CysH anions in this case are accommodated bilayer arrangement with the carboxyl of individual anions attaching alternately to the upper and lower hydroxide layers. There might be hydrogen bonding between mercapto of adjacent anions (–SH···SH–). The schematic representation of the probable arrangement for L-CysH / LDH (Sam 2) is shown in Fig. 3c.

Table 1 Chemical compositions for synthesized LDH materials

Sample	Chemical composition	Mg/Al molar ratio
L-Cys/LDH	$Mg_{4.04}Al_{2.00}(OH)_{12.08}(C_6H_{10}N_2O_4S_2)_{0.92}(NO_3)_{0.04}(CO_3)_{0.06} \cdot 3.98H_2O$	2.02
L-CysH/LDH (Sam1)	$Mg_{4.08}Al_{2.00}(OH)_{12.16}(C_3H_5NO_2S)_{0.72}(NO_3)_{0.48}(CO_3)_{0.04} \cdot 3.92H_2O$	2.04
L-CysH/LDH (Sam2)	$Mg_{4.02}Al_{2.00}(OH)_{12.04}(C_3H_6NO_2S)_{1.28}(NO_3)_{0.58}(CO_3)_{0.07} \cdot 3.50H_2O$	2.01

Chemical composition of L-Cys/LDH and L-CysH/LDH

Table 1 lists the chemical compositions of L-Cys/LDH and L-CysH/LDH (Sam 1 and Sam 2). It should be noted that the determination of chemical compositions of the intercalated materials are due to the results of elemental analysis, the rule of charge balance as well as the charge on the ion of the interlayer guests. The Mg^{2+}/Al^{3+} molar ratios in the materials are close to that of the Mg/Al input (2.00), indicating essentially complete coprecipitation of both metal ions. It can be seen from Table 1 that L-CysH/LDH (Sam 2) has the highest organic content among the three samples, due to its interlayer monovalent anion. Furthermore, some nitrate ions are also co-intercalated within the gallery spaces besides the guest in all the three intercalates. Similar observations regarding incomplete intercalation of amino acids into layered double hydroxides by coprecipitation have been reported by Whilton et al. [22] and Aisawa et al. [24]. Some Mg–Al–CO_3 LDH phase coexists with the intercalated materials, which is in consistent with the XRD results. The total exclusion of carbonate from the interlayer space of LDHs is known to be difficult, which can be readily explained on the basis of the favorable lattice stabilization enthalpy associated with the small and highly charged CO_3^{2-} anions [31].

Thermal decomposition studied by TG-DTA

The TG and DTA curves of the L-Cys/LDH are shown in Fig. 4(a, b, respectively). The thermal decomposition of the L-Cys/LDH is characterized by three weight loss steps: the first one from room temperature to 180 °C corresponds to the removal of surface adsorbed water (below about 100 °C) and interlayer water molecules; the second one (200–320 °C), involving a gradual weight loss, is the result of the decomposition of L-Cys ions and dehydroxylation of the brucite-like layers; the third one with a sharp weight loss in the temperature region 320–460 °C with a corresponding exothermic maximum at 480 °C in the DTA curve is due to dehydroxylation of the host layers as well as combustion of the interlayer decomposed materials.

Figure 5 displays the TG (a1, b1) and DTA (a2, b2) curves for the L-CysH/LDH (Sam 1 and Sam 2). There are also three weight loss steps during the thermal decomposition of the L-CysH/LDHs. The first one (20–150 °C) is due to loss of both adsorbed and interlayer water molecules; the second in the temperature region 180–350 °C involves two simultaneous processes—the decomposition of L-CysH anions and dehydroxylation of the brucite-like layers; the third stage (350–530 °C) can be attributed to dehydroxylation of the host layers as well as combustion of the decomposed materials, with the corresponding strong exothermic peak ob-

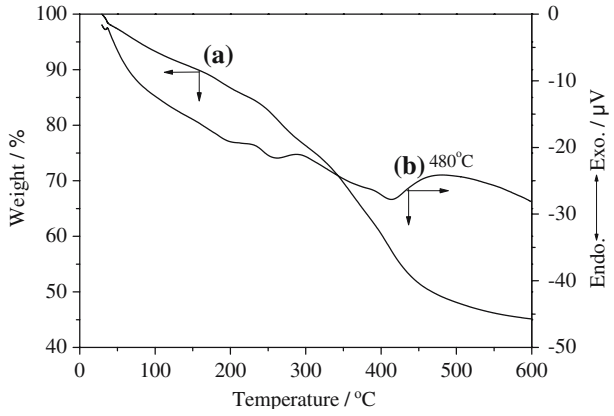

Fig. 4 Thermal analysis for L-Cys/LDH: (**a**) TG curve, (**b**) DTA curve

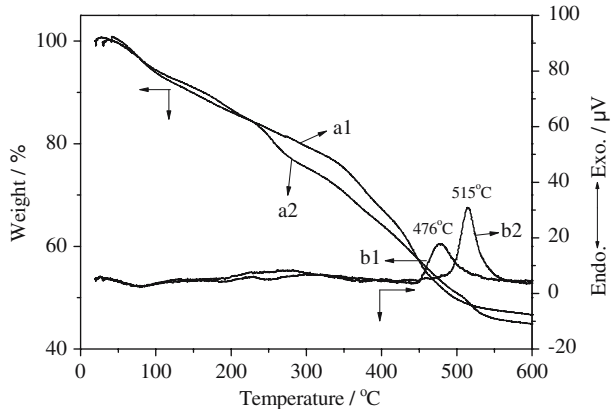

Fig. 5 Thermal analysis for L-CysH/LDH: (**a**1) TG curve for Sam 1, (**b**1) DTA curve for Sam1, (**a**2) TG curve for Sam 2, (**b**2) DTA curve for Sam 2

served at 476 (Sam 1) and 515 °C (Sam 2) in the DTA curves, respectively. The discrepancy of interlayer guest orientations and interactions between the two samples results in the different temperature of the exothermic peaks.

Conclusions

L-Cys/LDH and L-CysH/LDH have been obtained by the intercalation of L-Cys and L-CysH anions into Mg–Al layered double hydroxide by the method of coprecipitation and ion-exchange, respectively. XRD was used to confirm the intercalation structure, with d_{003} = 1.46 nm for L-Cys/LDH. In the case of L-CysH intercalated composites, two kinds of well-crystallized materials with different basal spacing (d_{003} = 1.03 and 1.44 nm, respectively) were obtained, which is due to different charge on the ion and orientation of the gallery anions as a result of different solution pH during preparation. This indicates that monovalent or bivalent L-CysH anions intercalated LDHs with different guest anion orientations can be obtained by the control of reaction conditions. The schematic models of the intercalation structures were proposed taking into account the length of the interlayer anion and the gallery height. TG-DTA analysis shows that there are three weight loss steps during the thermal decomposition of L-Cys/LDH and L-CysH/LDH in the temperature range 20–600 °C.

Acknowledgments This project was supported by the National Natural Science Foundation Major International Joint Research Program (Project No.: 20620130108), National Natural Science Foundation of China (Grant No.: 20601001), the Program for New Century Excellent Talents in University (Project No.: NCET-05-121) and the 111 Project (Project No.: B07004).

References

1. Meyn M, Beneke K, Lagaly G (1990) Inorg Chem 29:5201
2. Williams GR, Norquist AJ, O'hare D (2004) Chem Mater 16:975
3. Khan AI, Lei L, Norquist AJ, O'hare D (2001) Chem Commun 2342
4. Moujahid EM, Dubois M, Besse JP, Leroux F (2005) Chem Mater 17:373
5. Zhao HT, Vance GF (1998) Clays Clay Miner 46:712
6. Ding WP, Gu G, Zhong W, Zang WC, Du YW (1996) Chem Phys Lett 262:259
7. Newman SP, Jones W (1998) New J Chem 22:105
8. Constantino VRL, Pinnavaia TJ (1994) Catal Lett 23:361
9. Corma A, Fornes V, Rey F, Cervilla A, Llopis E, Ribera A (1995) J Catal 152:237
10. Ogawa M, Kuroda K (1995) Chem Rev 95:399
11. Tagaya H, Sato S, Kuwahara T, Kadokawa J, Masa K, Chiba K (1994) J Mater Chem 4:1907
12. Sels B, Vos DD, Buntinx M, Pireard F, Mesmaeker AK, Jacobs P (1999) Nature 400:855
13. Ukrainczyk L, Chibwe M, Pinnavaia TJ, Boyd SA (1995) Environ Sci Technol 29:439
14. Fogg AM, Green VM, Harvey HG, O'hare D (1999) Adv Mater 11:1466
15. Fogg AM, Dunn JS, Shyu SG, Cary DR, O'hare D (1998) Chem Mater 10:351
16. Fudala A, Palinko I, Hrivnak B, Kiricsi I (1999) J Therm Anal Calorim 56:317
17. Aisawa S, Takahashi S, Ogasawara W, Umersu Y, Narata E (2001) J Solid State Chem 162:52
18. Choy J, Kwak S, Park J, Jeong Y, Portier J (1999) J Am Chem Soc 121:1399
19. Kwak SY, Jeong YJ, Park JS, Choy JH (2002) Solid State Ionics 151:229
20. Hwang SH, Han YS, Choy JH (2001) Bull Korean Chem Soc 22:1019
21. Ambrogi V, Fardella G, Grandolini G, Perioli L (2001) Int J Pharm 220:23
22. Whilton NT, Vickers PJ, Mann S (1997) J Mater Chem 7:1623
23. Fudala A, Palinko I, Kiricsi I (1999) Inorg Chem 38:4653
24. Aisawa S, Takahashi S, Ogasawara W, Umetsu Y, Narita E (2001) J Solid State Chem 162:52
25. Shinitzky M, Nudelman F, Barda Y, Haimovitz R, Chen E, Deamer DW (2002) Origins Life Evol B 32:285
26. Vaysse C, Guerlou-Demourgues L, Delmas C (2002) Inorg Chem 41:6905
27. Cavani F, Trifiro F, Vaccari A (1991) Catal Today 11:173
28. Nakamoto K (1997) In: Infrared and Raman spectra of inorganic and coordination compounds. Wiley & Sons, New York
29. Prevot V, Forano C, Besse JP (1998) Inorg Chem 37:4293
30. Wang XC (2001) In: Biology chemistry. Tsinghua University Press, Beijing
31. Oriakhi CO, Farr IV, Lerner MM (1996) J Mater Chem 6:103